In-Situ Hydrothermal Synthesis of Oriented Hematite Nanorods for Sub-ppm Level Detection of Ozone Gas

Ariadne Catto, Sandrine Bernardini, Khalifa Aguir, Elson Longo, Luís da Silva

Journal of Alloys and Compounds xxx (xxxx) 169444

Contents lists available at ScienceDirect

Journal of Alloys and Compounds

journal homepage: www.elsevier.com/locate/jallcom

Research Article

In-situ hydrothermal synthesis of oriented hematite nanorods for sub-ppm level detection of ozone gas

Ariadne C. Catto [a,*], Sandrine Bernardini [b], Khalifa Aguir [b], Elson Longo [a], Luís F. da Silva [c]

[a] Center for the Development of Functional Materials (CDMF), Federal University of São Carlos, 13565-905 São Carlos, SP, Brazil
[b] Aix-Marseille Univ, CNRS, IM2NP Marseille, France
[c] Laboratory of Nanostructured Multifunctional Materials (LM2N), Federal University of São Carlos, 13565-905 São Carlos, SP, Brazil

ARTICLE INFO

Article history:
Received 15 January 2023
Received in revised form 15 February 2023
Accepted 24 February 2023

Keywords:
α-Fe2O3 nanorods
Resistive gas sensor
Ozone
Hydrothermal synthesis

ABSTRACT

The development of simple and reproducible synthesis techniques for obtaining one-dimensional semiconducting nanostructures is essential for the advancement of gas sensor devices. We report a facile and versatile approach for the in-situ growth of vertically oriented hematite nanorods to be applied as a resistive ozone gas sensor. The α-Fe_2O_3 nanorods were grown via a hydrothermal treatment directly onto an Al_2O_3 substrate with interdigitated Pt electrodes, thus facilitating the integration of nanorods into the sensing platform. At 150 °C, the gas-sensing experiments revealed a good sensitivity of these nanorods to different ozone concentrations (10–570 ppb), besides a fast response time and repeatable response–recovery cycles. The present study offers a promising way for designing high-performance gas sensors based on hematite nanorods.

1. Introduction

It is widely known that the presence of various chemical species dumped into the atmosphere, mainly resulting from industrial activities and fossil fuel burning, has affected both climatic conditions and human beings. For this reason, the World Health Organization (WHO) has warned the population about the importance of reducing the current levels of pollutants in the atmosphere [1].

Despite its usefulness as a disinfectant agent in water treatment processes and the food industry, ozone (O_3) gas is toxic even at very low levels [2]. As a strong oxidant, O_3 gas can cause damage to human cells and the lining fluids of the airways, leading to respiratory diseases [1,2] In this context, environment-friendly materials that are sensitive to certain noxious gases and working at mild temperatures appear as a good strategy.

According to literature, a variety of materials have been studied as ozone sensing layer, for example, WO_3, SnO_2, In_2O_3, ZnO, Ag_2WO_4, $NiCo_2O_4$, $ZnFe_2O_4$, $CuAlO_2$, $CsPbBr_3$, and β-In_2S_3 [3–8]. For instance, Ning Sui and co-works [9] obtained nanostructured In_2O_3 powders using a surfactant-assistant co-precipitation method and then annealed at 600 °C. They observed good sensitivity from 30 ppb of O_3 gas at working temperature of 70 ∘C. Lima and co-workers [10] investigated the ozone detection performance of rGO-ZnO nanocomposites obtained by a synthesis procedure based on a two-step physical process. The authors observed an improvement of sensor response from ppt-levels, at an operating temperature of 300 ∘C. Despite these achievements of O_3 gas sensors, the development of synthesis and processing methods that allow the integration of sensor materials into the gas sensor device, with reduced complexity remains a necessary challenge.

As above mentioned, the most widely used materials for the detection of (non-)toxic gases are semiconducting metal oxides (MOx), including hematite (α-Fe_2O_3), which stands out for being successfully applied as a resistive gas sensor. Hematite has gained increased attention due to its low- cost, high oxygen ion mobility on the material surface, excellent chemical and thermal stability under ambient atmosphere [11,12].

Table 1 summarizes some works devoted to the investigation of gas sensors based on hematite synthesized by different methods. Although chemical and physical routes have been used to obtain hematite, most of them are expensive and require high temperatures (> 200 °C) and longer synthesis times. With respect to the chemical methods, several processing steps are often required in addition to the deposition process for integrating particles into the sensing platform.

Several researchers have focused on simple, efficient and low-cost synthesis methods to obtain one-dimensional (1-D) materials. In this regard, the hydrothermal route has been widely used because it allows the fine-tuning of the material microstructure, design, and performance at the nanoscale for gas-sensing application [19]. Additionally, the possibility to grow 1D nanostructures directly onto the sensing platform is another advantage of this method [20].

* Corresponding author at: Center for the Development of Functional Materials (CDMF), Federal University of São Carlos, 13565-905 São Carlos, SP, Brazil.
E-mail address: ade.catto@gmail.com (A.C. Catto).

https://doi.org/10.1016/j.jallcom.2023.169444
0925-8388/© 20XX

Table 1
Summary of the results obtained with gas sensors based on hematite synthesized by different methods.

Method of synthesis	Synthesis temperature	Gas target	Ref.
Hydrothermal method	200 °C	BTEX	[13]
Hydrothermal method	200 °C	O_3	[14]
Radio-frequency (R.F.) sputtering	700–1000 °C	O_3 and NO_2	[15]
Sol-gel route *	243–550 °C	NO_2	[16]
Plasma enhanced chemical vapor deposition (PECVD)	80–350 °C	i-C_4H_{10}, CO and CH_4	[17]
Hydrothermal method	180 °C	NH_3 and VOCs	[18]

* Under super critical conditions of ethanol (Pc = 63.6 bars).

Motivated by these considerations, we report the in-situ synthesis of hierarchical 1-D α-Fe_2O_3 nanorod-like structures to be used as a resistive ozone gas sensor. The hematite nanorods were directly grown onto an Al_2O_3/Pt substrate via a hydrothermal method. X-ray diffraction measurements and X-ray photoelectron spectroscopy confirmed the presence of the hematite phase. FE-SEM images revealed the preferential growth of the rod-like structures along the perpendicular (c-axis) direction. Electrical measurements demonstrated the efficiency of the hematite nanorods, which exhibited a good sensitivity to sub-ppm ozone levels at 150 °C with a complete recovery. To the best of our knowledge, this is the first time that a facile hydrothermal process is used for directly growing 1-D hematite nanorods onto a sensing platform for application as an ozone gas sensor.

2. Experimental section

2.1. Sample preparation

The highly oriented α-Fe_2O_3 nanorod arrays were grown directly onto an Al_2O_3 substrate with interdigitated Pt electrodes via a hydrothermal method. First, $FeCl_3$0.6 H_2O (Aldrich, ≥99.9%) and $NaNO_3$ (Aldrich, ≥ 99.0%) were dissolved in 80 ml of deionized water under constant stirring for 30 min at room temperature, in a concentration of 0.15 M and 1 M. Afterwards, the precursor solution was placed in screw-capped glass bottle (SCGB) and the substrate surface with interdigitated Pt electrodes was placed face down on the bottom of the SCGB. Fig. S1 presents a schematic illustration of the SCGB used to obtain the hematite nanorods grown onto a sensing platform. Then, the SCGB was placed in an electric furnace preheated to 100 °C for 6 h. At the end of the hydrothermal treatment, the substrate was then removed from the solution, and washed with deionized water and isopropyl alcohol. Afterwards, the film was submitted to a thermal treatment at 400 °C for 1 h at a heating rate of 10 °C.min^{-1}.

2.2. Characterization techniques

The crystalline phase of the hematite structures was examined at room temperature by X-ray diffraction using a Shimadzu diffractometer (XRD6100, CuKα radiation) in the 2θ range from 20° to 80° with a step of 0.02 and at a scanning speed of 2° min^{-1}. Top-view and cross-section images of the samples were analyzed on a field emission scanning electron microscope (FE-SEM, Zeiss Supra35). X-ray photoelectron spectroscopy (XPS) measurements were performed on a Scienta Omicron spectrometer model ESCA + using monochromatic AlKα (1486.6 eV) radiation. The binding energies obtained were corrected for specimen charging by referencing the adventitious carbon located at 284.8 eV. The data were analyzed using CasaXPS software.

2.3. Sensing experiments

The hematite sensor sample was inserted into a special chamber that allows the control of the substrate temperature and the gas flows. The different O_3 gas levels were generated using a calibrated pen-ray UV lamp. In these experiments, the dry air containing O_3 gas was blown directly onto the sample, keeping a constant flow of 500 SCCM. Further details about the gas-sensing workbench can be found in previous works published by our team [14,21]. Also, the sensing performance of the sample was evaluated to four NH_3 levels (5, 10, 50 and 100 ppm). In these measurements, the electrical resistance of the sample was monitored with an electrometer (Keithley, 6514) by applying a voltage of 1 V (*DC*). The sensor response (S) was defined as $S = R_{O3}/R_{air}$, where R_{O3} and R_{air} are the electric resistance of the sensor exposed to O_3 gas and dry air [14]. The response and recovery times were estimated following a procedure reported elsewhere [8,14].

3. Results and discussion

The X-ray diffraction pattern of the α-Fe_2O_3 nanorods is shown in Fig. S2. It can be seen that all XRD reflections correspond to the hematite crystalline phase with a rhombohedral structure (JCPDS card No. 87–1164). From the SEM micrographs, Fig. 1(a-b), it can be verified that the hydrothermal method resulted in vertically aligned rod-like α-Fe_2O_3 structures, with an average length and diameter of 460 nm and 60 nm.

It is worth mentioning that unlike what was observed by Ferraz and co-workers [22], who grew hematite nanorods onto an FTO substrate, our structures grown onto an Al_2O_3 substrate exhibited a less orientational texture. This behavior may be attributed to the absence of a seed layer and the position of the substrate during the hydrothermal treatment. In our previous work, we obtained also by a hydrothermal method well vertically-oriented ZnO nanorods that grew onto a crystalline ZnO film [20].

Fig. S3 shows the XPS survey spectra of the α-Fe_2O_3 nanorods grown onto a Al_2O_3/Pt substrate. All electronic transitions revealed the presence of Fe and O. A quantitative analysis of the survey spectra and

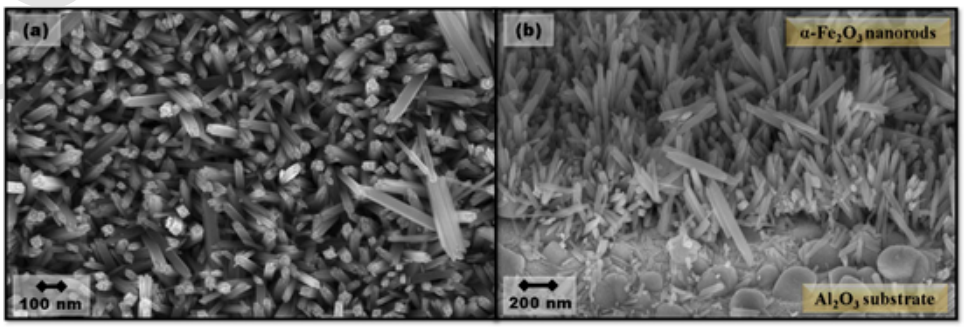

Fig. 1. FE-SEM images of α-Fe_2O_3 nanorods. (a) Surface microstructure and (b) cross-section.

the O 1 s region allowed us to estimate the atom ratio of Fe:O, i.e., 0.66. The atomic concentration of Fe and O determined from the survey spectra was 88.9% and 11.1%. To calculate the Fe/O ratio, only the oxygen species associated with Fe-O bonds were considered from the analysis of the O 1 s high-resolution spectrum, resulting in 16.7% of oxygen species related to α-Fe_2O_3 phase and 83.3% of adsorbed oxygen species from the atmosphere. The high-resolution Fe 2p XPS spectra (Fig. 2a) reveals two main peaks at 710.8 and 724.3 eV consistent with Fe 2p3/2 and Fe 2p1/2 levels, indicating the presence of Fe^{3+} ions on the α-Fe_2O_3 surface [23–25].

Fig. 2(b) shows the O 1 s spectrum of the α-Fe_2O_3 nanorods deconvoluted into two components at 529.6 eV and 531.1 eV [26]. These components are assigned to oxygen species (O^{2-}) located in the lattice bound to the metal cations and adsorbed hydroxyl groups. According to the literature, the component at about 531.5 eV has also been linked to oxygen vacancies or defects [27,28]. The performance of gas sensors based on MOXs is ruled by surface reactions. As a result, the control of surface defects has been an efficient strategy for enhancing sensing performance. Cao and co-workers [29] conducted an in-situ Raman spectroscopy study to understand the oxygen vacancy-dependent gas-sensing mechanism of α-Fe_2O_3 for acetone detection. They found that the intensity and FWHM peaks as well as the scattering frequencies of the corresponded Raman scattering signals of α-Fe_2O_3 underwent substantial alterations when the α-Fe_2O_3 was exposed to acetone. The obtained results suggested that the gas-sensing reaction is related to the adsorption of oxygen species at the oxygen vacancy site [29].

Regarding the ozone gas-sensing performance of the hematite nanorods, Fig. 3 reveals the relationship between operating temperature and sensing performance towards 163 ppb of O_3 level. As it can be seen, the sensing activity increases as a function of working temperature, reaching a maximum at 150 °C followed by a decrease at 250 °C. The ozone sensor response remained slightly unchanged in the range of 150–250 °C. Concerning the response and recovery times, there was a pronounced reduction of these values up to 150 °C, as observed in Fig. 3 (b).

Fig. 4 presents the real-time monitoring of the α-Fe_2O_3 nanorods when exposed to a constant ozone level of 10 ppb at different time intervals and a constant working temperature of 150 °C. It can be seen that the magnitude of change in resistance increases at longer exposure times to O_3 gas, reaching full recovery after each cycle. No evidence of saturation linked to the high surface area to volume ratio of the rod-like structures was observed [20].

Fig. 5 shows the sensor response of the α-Fe_2O_3 nanorods as a function of O_3 gas concentration at 150 ºC. As verified, the nanorods have good response repeatability along with total recovery, since after consecutive exposure cycles, the sample was able to detect a lower ozone level (10 ppb). Moreover, there was an increase in sensor response with O_3 gas concentration, showing a saturation tendency from 163 ppb (inset in Fig. 5). This behavior suggests that the sensor surface was

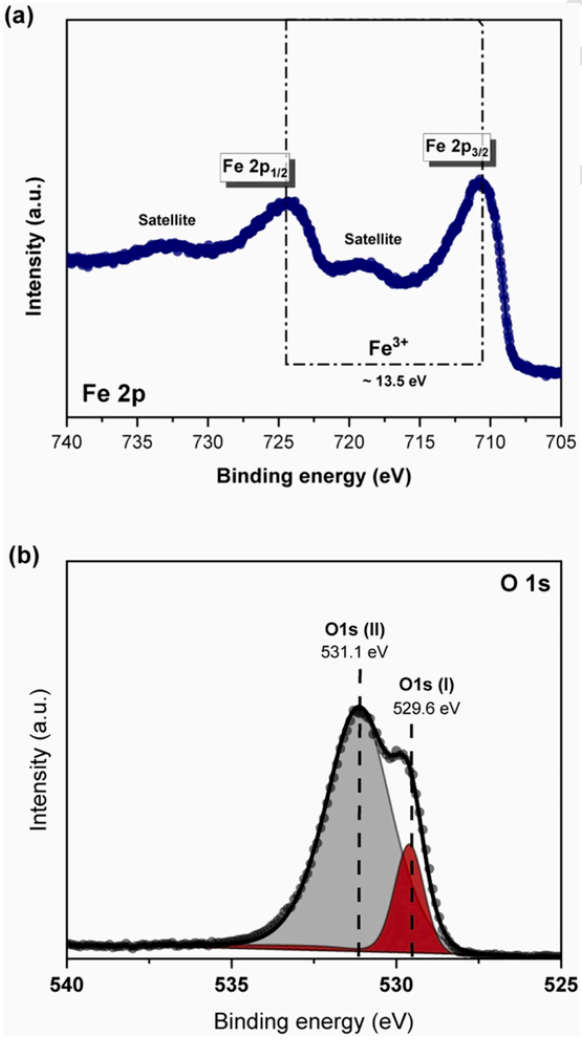

Fig. 2. XPS spectra of the as-prepared α-Fe_2O_3 nanorods. (a) Fe 2p and (b) O 1 s.

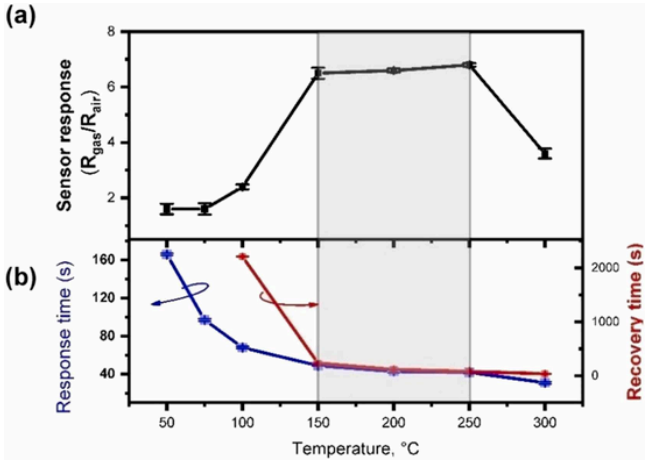

Fig. 3. As-prepared α-Fe_2O_3 nanorods exposed to 163 ppb O_3 as a function of working temperature. (a) Sensor response and (b) response and recovery times.

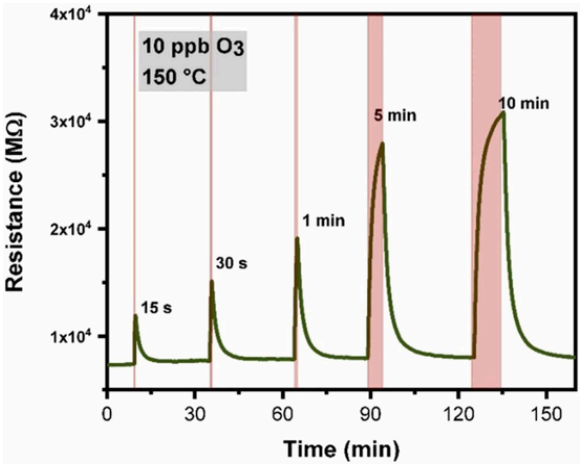

Fig. 4. Ozone gas-sensing response of α-Fe_2O_3 nanorods exposed to 10 ppb at a working temperature of 150 ºC and five different exposure times.

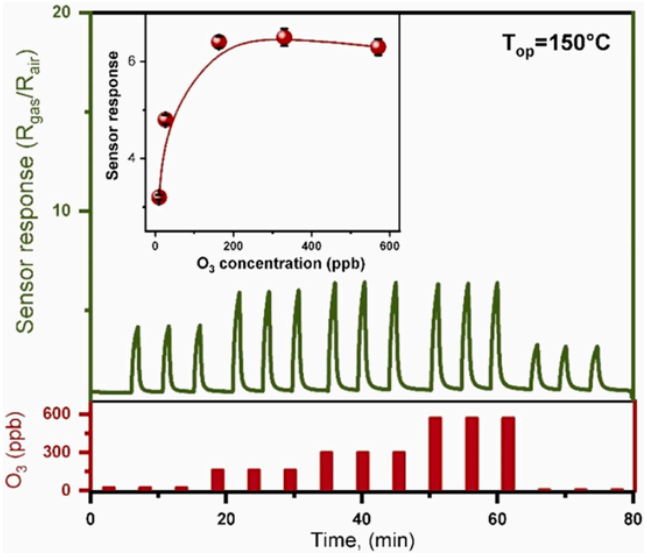

Fig. 5. Dynamic response-recovery curves of α-Fe_2O_3 nanorods exposed to five different O_3 gas levels (26, 163, 300, 570 and 10 ppb) at 150 ∘C. The inset shows the sensing response as a function of O_3 gas concentration.

fully covered and that there were not enough adsorption sites available to react with O_3 molecules at higher concentrations. According to the WHO Global air quality guidelines, the recommended exposure to ozone gas is an average concentration of 50 ppb for 8 h. Therefore, as the α-Fe_2O_3 nanorods exhibited a detection limit below this value, it can be concluded that these structures have practical application as an ozone gas sensor.

The long-term stability to ozone gas and the sensing response of the α-Fe_2O_3 nanorods to a reducing gas were also investigated, and the results are displayed in Fig. 6. Fig. 6(a) shows the long-term stability of the α-Fe_2O_3 nanorods exposed 10 ppb O_3 gas at 150 °C, in a period of 3 weeks. The stability and repeatability were evaluated by exposing the nanorods to sequential gas sensing tests every 7 days (Fig S4). It can be seen that hematite nanorods exhibited good stability and repeatable characteristic during the evaluation period. Furthermore, to verify the sensitivity of the nanorods to a reducing gas, they were exposed to four NH_3 concentrations (5, 10, 50 and 100 ppm) at a working temperature of 150 °C, as seen in Fig. S5. Despite detecting all NH_3 levels investigated, the response of the nanorods to the highest O_3 level (0.57 ppm) was higher in comparison to the lowest NH_3 level (5 ppm) available in our workbench, as displayed in Fig. 6(b).

These results presented herein clearly confirm the potential of the synthesis approach used for obtaining the hematite nanorods as well as the promising sensing performance of these structures for the detection of sub-ppm levels of O_3 gas. Among the further experiments that will still be carried out is the evaluation of the stability and selectivity of the sensor in relation other interferents, mainly the influence of relative humidity.

4. Conclusions

This manuscript addresses a facile approach to obtain an ozone gas sensor based on hematite nanorods grown directly onto a sensing platform via a hydrothermal route. XRD and FE-SEM analyses revealed the presence of a single phase, i.e., hematite phase with rhombohedral structure, with the nanorods oriented along the c-axis. Gas-sensing measurements demonstrated that the hematite nanorods were sensitive to sub-ppm ozone levels at a mild temperature, showing total recovery. To the best of our knowledge, this is the first time that a hydrothermal process was used to grow 1-D hematite nanorods directly onto a sensing platform for application as an ozone gas sensor.

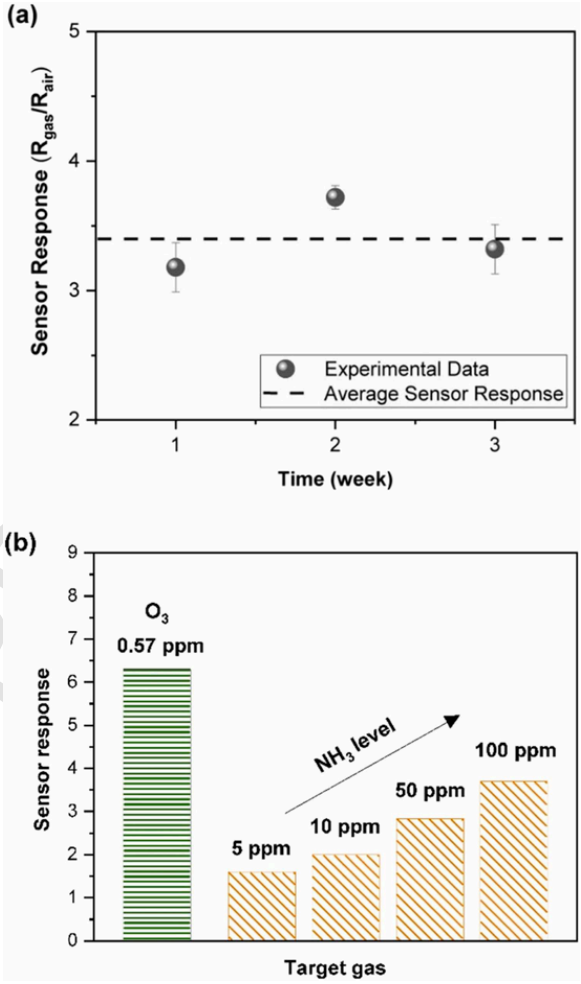

Fig. 6. Gas-sensing properties of α-Fe_2O_3 nanorods at 150 °C. (a) Stability during 3 weeks exposed to 10 ppb of ozone, and (b) comparison of the response to O_3 and NH_3 gases.

CRediT authorship contribution statement

Ariadne C. Catto : Conceptualization, Methodology, Data curation, Writing – original draft, Investigation, Writing – review & editing. **Sandrine Bernardini :** Data curation, Writing – review & editing. **Khalifa Aguir :** Writing – review & editing. **Elson Longo :** Supervision, Writing – review & editing. **Luís F. da Silva :** Investigation, Methodology, Data curation, Supervision, Writing – review & editing.

Declaration of Competing Interest

The authors declare that they have no known competing financial interests or personal relationships that could have appeared to influence the work reported in this paper.

Data Availability

No data was used for the research described in the article.

Acknowledgements

This research was partially performed at the Brazilian Nanotechnology National Laboratory (LMF-18580), Campinas, SP, Brazil. The authors acknowledge the financial support of the following Brazilian research funding institutions: FAPESP (under grants Nos. 2021/12684-8,

2018/18208-0, 2022/02927-3, 2021/07214-4 and 2013/07296-2) and CNPq (under grants Nos. 405140/2018-5, 426511/2018-2, and 310170/2021-4).

Appendix A. Supporting information

Supplementary data associated with this article can be found in the online version at doi:10.1016/j.jallcom.2023.169444.

References

[1] W. Avansi, A.C. Catto, L.F. da Silva, T. Fiorido, S. Bernardini, V.R. Mastelaro, K. Aguir, R. Arenal, One-dimensional V2O5/TiO2 heterostructures for chemiresistive ozone sensors, ACS Appl. Nano Mater. 2 (2019) 4756–4764, https://doi.org/10.1021/acsanm.9b00578.

[2] M.A. Zoran, R.S. Savastru, D.M. Savastru, M.N. Tautan, Assessing the relationship between ground levels of ozone (O_3) and nitrogen dioxide (NO_2) with coronavirus (COVID-19) in Milan, Italy, Sci. Total Environ. 740 (2020) 140005, https://doi.org/10.1016/j.scitotenv.2020.140005.

[3] K. Brintakis, E. Gagaoudakis, A. Kostopoulou, V. Faka, A. Argyrou, V. Binas, G. Kiriakidis, E. Stratakis, Ligand-free all-inorganic metal halide nanocubes for fast{,} ultra-sensitive and self-powered ozone sensors, Nanoscale Adv. 1 (2019) 2699–2706, https://doi.org/10.1039/C9NA00219G.

[4] S. Thirumalairajan, V.R. Mastelaro, C.A.J. Escanhoela, In-depth understanding of the relation between $CuAlO_2$ particle size and morphology for ozone gas sensor detection at a nanoscale level, ACS Appl. Mater. Interfaces 6 (2014) 21739–21749, https://doi.org/10.1021/am507158z.

[5] R. Souissi, N. Bouguila, M. Bendahan, K. Aguir, T. Fiorido, M. Abderrabba, I. Halidou, A. Labidi, Ozone sensing study of sprayed β-In2S3 thin films, J. Alloy. Compd. 900 (2022) 163513, https://doi.org/10.1016/j.jallcom.2021.163513.

[6] L.F. da Silva, A.C. Catto, W. Avansi Jr, L.S. Cavalcante, J. Andres, K. Aguir, V.R. Mastelaro, E. Longo, A novel ozone gas sensor based on one-dimensional (1D) α-Ag_2WO_4 nanostructures, Nanoscale 6 (2014) 4058–4062, https://doi.org/10.1039/C3NR05837A.

[7] R. Cristina de Oliveira, R.A. Pontes Ribeiro, G.H. Cruvinel, R.A. Ciola Amoresi, M.H. Carvalho, A.J. Aparecido de Oliveira, M. Carvalho de Oliveira, S. Ricardo de Lazaro, L. Fernando da Silva, A.C. Catto, A.Z. Simões, J.R. Sambrano, E. Longo, Role of surfaces in the magnetic and ozone gas-sensing properties of $ZnFe_2O_4$ nanoparticles: theoretical and experimental insights, ACS Appl. Mater. Interfaces 13 (2021) 4605–4617, https://doi.org/10.1021/acsami.0c15681.

[8] Y.J. Onofre, A.C. Catto, S. Bernardini, T. Fiorido, K. Aguir, E. Longo, V.R. Mastelaro, L.F. da Silva, M.P.F. de Godoy, Highly selective ozone gas sensor based on nanocrystalline $Zn_{0.95}Co_{0.05}O$ thin film obtained via spray pyrolysis technique, Appl. Surf. Sci. 478 (2019) 347–354, https://doi.org/10.1016/j.apsusc.2019.01.197.

[9] N. Sui, P. Zhang, T. Zhou, T. Zhang, Selective ppb-level ozone gas sensor based on hierarchical branch-like In_2O_3 nanostructure, Sens. Actuators B Chem. 336 (2021) 129612, https://doi.org/10.1016/j.snb.2021.129612.

[10] B.S. de Lima, A.A. Komorizono, W.A.S. Silva, A.L. Ndiaye, J. Brunet, M.I.B. Bernardi, V.R. Mastelaro, Ozone detection in the ppt-level with rGO-ZnO based sensor, Sens. Actuators B Chem. 338 (2021) 129779, https://doi.org/10.1016/j.snb.2021.129779.

[11] A. Mirzaei, B. Hashemi, K. Janghorban, α-Fe_2O_3 based nanomaterials as gas sensors, J. Mater. Sci. Mater. Electron 27 (2016) 3109–3144, https://doi.org/10.1007/s10854-015-4200-z.

[12] D.H. Kim, Y.-S. Shim, J.-M. Jeon, H.Y. Jeong, S.S. Park, Y.-W. Kim, J.-S. Kim, J.-H. Lee, H.W. Jang, Vertically ordered hematite nanotube array as an ultrasensitive and rapid response acetone sensor, ACS Appl. Mater. Interfaces 6 (2014) 14779–14784, https://doi.org/10.1021/am504156w.

[13] L.F. da Silva, A.C. Catto, S. Bernardini, T. Fiorido, J.V.N. de Palma, W. Avansi, K. Aguir, M. Bendahan, BTEX gas sensor based on hematite microrhombuses, Sens. Actuators B Chem. 326 (2021) 128817, https://doi.org/10.1016/j.snb.2020.128817.

[14] A.C. Catto, M.C. Oliveira, R.A.P. Ribeiro, W. Avansi, L.F. da Silva, E. Longo, Hematite rhombuses for chemiresitive ozone sensors: experimental and theoretical approaches, Appl. Surf. Sci. 563 (2021) 150209, https://doi.org/10.1016/j.apsusc.2021.150209.

[15] M. Debliquy, C. Baroni, A. Boudiba, J.-M. Tulliani, M. Olivier, C. Zhang, Sensing characteristics of hematite and barium oxide doped hematite films towards ozone and nitrogen dioxide, Procedia Eng. 25 (2011) 219–222, https://doi.org/10.1016/j.proeng.2011.12.054.

[16] M. Hjiri, Highly sensitive NO2 gas sensor based on hematite nanoparticles synthesized by sol–gel technique, J. Mater. Sci. Mater. Electron 31 (2020) 5025–5031, https://doi.org/10.1007/s10854-020-03069-4.

[17] E.-T. Lee, G.-E. Jang, C.K. Kim, D.-H. Yoon, Fabrication and gas sensing properties of α-Fe_2O_3 thin film prepared by plasma enhanced chemical vapor deposition (PECVD), Sens. Actuators B Chem. 77 (2001) 221–227, https://doi.org/10.1016/S0925-4005(01)00716-X.

[18] Y. Tao, Q. Gao, J. Di, X. Wu, Gas sensors based on alpha-Fe_2O_3 nanorods, nanotubes and nanocubes, J. Nanosci. Nanotechnol. 13 (2013) 5654–5660, https://doi.org/10.1166/jnn.2013.7559.

[19] C. Dong, R. Zhao, L. Yao, Y. Ran, X. Zhang, Y. Wang, A review on WO3 based gas sensors: morphology control and enhanced sensing properties, J. Alloy. Compd. 820 (2020) 153194, https://doi.org/10.1016/j.jallcom.2019.153194.

[20] A.C. Catto, L.F. Da Silva, C. Ribeiro, S. Bernardini, K. Aguir, E. Longo, V.R. Mastelaro, An easy method of preparing ozone gas sensors based on ZnO nanorods, RSC Adv. 5 (2015) 19528, https://doi.org/10.1039/c5ra00581g.

[21] D.A. Mirabella, P.M. Desimone, M.A. Ponce, C.M. Aldao, L.F. da Silva, A.C. Catto, E. Longo, Effects of donor density on power-law response in tin dioxide gas sensors, Sens. Actuators B Chem. 329 (2021) 129253, https://doi.org/10.1016/j.snb.2020.129253.

[22] L.C.C. Ferraz, W.M.J. Carvalho, D. Criado, F.L. Souza, Vertically oriented iron oxide films produced by hydrothermal process: effect of thermal treatment on the physical chemical properties, ACS Appl. Mater. Interfaces 4 (2012) 5515–5523, https://doi.org/10.1021/am301425e.

[23] P.S. Bagus, C.J. Nelin, C.R. Brundle, B.V. Crist, N. Lahiri, K.M. Rosso, Combined multiplet theory and experiment for the Fe 2p and 3p XPS of FeO and Fe_2O_3, J. Chem. Phys. 154 (2021) 94709, https://doi.org/10.1063/5.0039765.

[24] Y. Zheng, X. Zhang, J. Zhao, P. Yang, Assembled fabrication of α-Fe_2O_3/BiOCl heterojunctions with enhanced photocatalytic performance, Appl. Surf. Sci. 430 (2018) 585–594, https://doi.org/10.1016/j.apsusc.2017.06.097.

[25] X.-F. Lu, X.-Y. Chen, W. Zhou, Y.-X. Tong, G.-R. Li, α-Fe2O3@PANI core–shell nanowire arrays as negative electrodes for asymmetric supercapacitors, ACS Appl. Mater. Interfaces 7 (2015) 14843–14850, https://doi.org/10.1021/acsami.5b03126.

[26] X. Deng, J. Lee, C. Wang, C. Matranga, F. Aksoy, Z. Liu, Reactivity differences of nanocrystals and continuous films of α-Fe_2O_3 on Au(111) studied with in situ X-ray photoelectron spectroscopy, J. Phys. Chem. C. 114 (2010) 22619–22623, https://doi.org/10.1021/jp1085697.

[27] J. Lee, Y. Choi, B.J. Park, J.W. Han, H.-S. Lee, J.H. Park, W. Lee, Precise control of surface oxygen vacancies in ZnO nanoparticles for extremely high acetone sensing response, J. Adv. Ceram. 11 (2022) 769–783, https://doi.org/10.1007/s40145-022-0570-x.

[28] M. Al-Hashem, S. Akbar, P. Morris, Role of oxygen vacancies in nanostructured metal-oxide gas sensors: a review, Sens. Actuators B Chem. 301 (2019) 126845, https://doi.org/10.1016/j.snb.2019.126845.

[29] Z. Cao, Z. Jiang, L. Cao, Y. Wang, C. Feng, C. Huang, Y. Li, Lattice expansion and oxygen vacancy of α-Fe_2O_3 during gas sensing, Talanta 221 (2021) 121616, https://doi.org/10.1016/j.talanta.2020.121616.